Journal of Translational Medicine

RESEARCH

Open Access

Cancer-associated fibroblasts induce almonertinib resistance in non-small cell lung cancer

Guohao Wei[1†], Yu Nie[1†], Min Sun[1], Wenzheng Zhou[1], Huihui Zhao[1,3*], Fangfang Chen[2*] and Chuandong Zhu[1*]

Abstract

Background Almonertinib is the initial third-generation EGFR-TKI in China, but its resistance mechanism is unknown. Cancer-associated fibroblasts (CAFs) are essential matrix components in the tumor microenvironment, but their impact on almonertinib resistance is unknown. This study aimed to explore the correlation between CAFs and almonertinib resistance in non-small cell lung cancer (NSCLC).

Methods The anti-cancer effects of almonertinib on NSCLC cells, as well as the reversal of these effects mediated by CAFs, were validated through phenotypic experiments. Differential gene expression analysis, along with GO and KEGG enrichment analyses, was performed to predict the potential mechanisms underlying resistance to third-generation EGFR-TKIs. Finally, qPCR and Western blot analyses were used to explore the signaling pathways by which CAFs induce resistance to almonertinib in NSCLC cells.

Results Our findings revealed that almonertinib significantly suppressed the invasion, migration, and proliferation of EGFR T790M-mutant NSCLC cells. TGF-β1 successfully induced the differentiation of CAFs and upregulated the expression of CAF markers, including α-SMA and fibroblast activation protein (FAP). Exposure of H1975 cells to almonertinib increased TGF-β1 secretion. Additionally, CAFs enhanced the survival of almonertinib-treated NSCLC cells, whereas normal fibroblasts (NFs) exerted the opposite effect. qPCR analysis demonstrated that the expression of the core molecules of the Hippo pathway, YAP and TAZ, was lower in A549 cells than in H1975 cells, and CAF intervention further reduced YAP/TAZ expression in H1975 cells. Western blot analysis confirmed a significant reduction in YAP/TAZ protein levels in cancer cells treated with CAF-conditioned medium (CAF-CM) compared to those treated with normal control-conditioned medium (NC-CM). Finally, we demonstrated that CAFs induced resistance to almonertinib in NSCLC cells, potentially through a mechanism involving YAP/TAZ.

†Guohao Wei and Yu Nie contributed equally to this work.

*Correspondence:
Huihui Zhao
zhaohh1981@njucm.edu.cn
Fangfang Chen
longysh@163.com
Chuandong Zhu
zhucd@njucm.edu.cn

Full list of author information is available at the end of the article

Conclusion This study demonstrated that H1975 cells stimulated by almonertinib promoted the accumulation of CAFs in NSCLC cells, likely through increased secretion of TGF-β1. The accumulation of CAFs enhanced the survival of NSCLC cells undergoing almonertinib treatment and induced drug resistance. Additionally, the mechanism underlying CAF-induced drug resistance in NSCLC cells was potentially linked to the activation of the YAP/TAZ signaling pathway.

Keywords Cancer-associated fibroblasts, Non-small cell lung cancer, Almonertinib, Resistance

Introduction

Lung cancer was a leading cause of cancer-related mortality worldwide, characterized by the highest mortality rate and a high incidence [1]. Non-small cell lung cancer (NSCLC) represented the most prevalent subtype of lung cancer. Clinical treatments for NSCLC primarily included surgery, chemotherapy, radiotherapy, immunotherapy, and targeted therapy [2]. Because the early symptoms of NSCLC are not obvious and there is a lack of clear biomarkers, early diagnosis poses challenges. Patients are frequently diagnosed at an advanced stage, rendering drastic treatment dependent on more than surgical excision. Drug-assisted therapy is often used in combination with this treatment.

Mutations affecting the epidermal growth factor receptor (EGFR) gene are prevalent functional gene alterations in NSCLC, particularly in Asian populations. Approximately 50% of Asian patients have EGFR mutations in somatic cells [3]. Patients with this mutation can be treated with tyrosine kinase inhibitors (TKIs) targeting EGFR. First- and second-generation EGFR-TKIs have been listed successively, and great progress has been made in their clinical treatment. However, post-treatment drug resistance is a major problem, and secondary EGFR mutations are the main cause, among which T790M is the most common drug resistance mutation [4]. Third-generation EGFR-TKIs, such as osimertinib and almonertinib, are designed for T790M-resistant EGFR mutations. However, third-generation EGFR-TKIs also cause drug resistance in clinical settings. The mechanism of resistance to osimertinib in third-generation TKIs is complex and includes triple EGFR mutations, MET amplification, and histological phenotypic changes, but 40–50% of the mechanisms are still unknown [5].

Almonertinib, the first domestically developed third-generation EGFR-TKI, was approved for listing in March 2020 and is currently being used clinically [6]. Almonertinib covalently and irreversibly binds to the C797 residue in the EGFR tyrosine kinase-binding domain to induce apoptosis in NSCLC cells [7]. Currently, research on almonertinib has focused mainly on its clinical application, and few studies have explored the mechanism of its drug resistance. Drug resistance problems in the treatment of EGFR-TKIs cannot be avoided; therefore, there is an urgent need to study resistance to almonertinib in NSCLC.

Cancer-associated fibroblasts (CAFs), the most abundant stromal cell type within the tumor microenvironment, were derived from normal fibroblasts, epithelial cells, endothelial cells, or mesenchymal stem cells [8]. After CAFs are activated, phenotype transformation and the expression of their markers, such as alpha smooth muscle actin (α-SMA) and fibroblast activation protein (FAP), are upregulated. Different subtypes of CAFs have been shown to be related to negative outcomes in patients with gastric cancer, colon cancer, NSCLC, and various other malignancies [9–11]. CAFs are major sources of cytokines and chemokines. For example, hepatocyte growth factor (HGF) is a MET ligand, and the abnormal expansion of the MET proto-oncogene is an important mechanism underlying EGFR-TKI resistance. HGF secreted by CAFs binds to c-Met on the surface of tumor cells and activates intracellular HGF/c-Met-related signaling pathways, which are related to tumor radiotherapy, chemotherapy, and gefitinib resistance [12–14]. However, the relationship between CAFs and resistance to the third-generation EGFR-TKI almonertinib is unclear.

This study explored the importance of cancer-associated fibroblasts (CAFs) in the resistance of NSCLC cells to almonertinib. The GEO database was utilized to predict the signaling pathways potentially associated with almonertinib resistance, and the possible mechanism by which CAFs are involved in almonertinib resistance was preliminarily explored.

Materials and methods

Cell culture and reagents

The NSCLC cell lines H1975 (EGFR T790M mutant type) and A549 (EGFR wild-type), normal lung epithelial cells Beas-2B (wild-type EGFR), and human embryonic lung fibroblasts (HFL1) were purchased from the Shanghai Cell Bank. H1975 cells were cultured in RPMI 1640 medium (Cat. No. KGM31800–500; KeyGEN Biotech Co., Ltd.) supplemented with 10% fetal bovine serum (FBS) and 1% penicillin–streptomycin. A549 cells were cultured in F12K medium (Cat. No. ZQ-599; Shanghai Zhong Qiao Xin Zhou Biotechnology Co., Ltd.) supplemented with 10% FBS and 1% penicillin–streptomycin, whereas HFL1 cells were cultivated in media supplemented with 15% FBS. Beas-2B cells were cultivated in DMEM (Cat. No. KGM12800–500; KeyGEN Biotech

Co., Ltd.) supplemented with 10% FBS and 1% penicillin–streptomycin. Almonertinib was provided by Jiangsu Hansoh Pharmaceutical Group Co., Ltd. Human recombinant protein TGF-β1 (Cat. No. 10804-H08H) was purchased from Sino Biological, Inc.

Cell counting Kit-8 (CCK-8) assay

Cells were seeded into 96-well plates at a density of 5,000 cells per well. Various concentrations of the drug (0, 2, 4, 8, 16, and 32 μM) were added to the culture medium, and the cells were incubated for 24, 48, and 72 h. Following treatment, 10 μL of CCK-8 solution (Cat. No. BS350C; Labgic Technology Co., Ltd.) was added to each well and incubated at 37 °C. Optical density at 450 nm (OD450) was measured using a Multiskan GO plate reader.

Colony formation assay

Cells were seeded into 6-well plates at a density of 2000 cells per well and incubated for 24 h. The medication-containing substance was then replaced. After an additional 24 h, the medium supplemented with 10% FBS was replaced, and the cells were cultured for 7–10 days. Subsequently, 500 μL of 4% paraformaldehyde solution was added to each well for fixation for 20 min, followed by the addition of 500 μL of 1% crystal violet solution for staining for another 20 min. Stained colonies were recorded and analyzed.

Transwell migration and invasion assays

The cell density was adjusted to 2.5×10^5/mL. The cell suspension (200 μL) was introduced into the upper chamber of a Transwell insert, whereas medium supplemented with 10% FBS was added to the lower chamber. After 24 h of cultivation, 500 μL of 4% polymerization solution was added for 20 min of fixation, followed by the addition of 500 μL of 1% crystal violet solution for an additional 20 min. Transwell invasion assays were performed via Matrigel-coated inserts via the same steps described above.

Western blot

Proteins were extracted by digesting the cells with RIPA buffer supplemented with PMSF. Protein concentrations were determined using a BCA protein assay kit (Catalog No. P0012, Beyotime Biotech Co., Ltd.). The extracted proteins were separated via sodium dodecyl sulfate–polyacrylamide gel electrophoresis (SDS-PAGE) and transferred onto PVDF membranes. The membranes were blocked with 5% skim milk for 2 h and incubated overnight with primary antibodies. Afterward, the membranes were incubated with secondary antibodies for 1 h. Protein bands were detected using a super ECL prime kit (Catalog No. PS6008, Proteinbio Biotech Co., Ltd.). The following antibody dilutions were used: anti-GAPDH (1:10000, ABclonal), anti-αSMA (1:4000, Proteintech), anti-FAP (1:1000, ABclonal), HRP-conjugated secondary antibody (1:10000, ABclonal), anti-YAP/TAZ (1:1000, CST), and anti-GAPDH (1:50000, ABclonal).

Enzyme-linked immunosorbent assay (ELISA)

The cell supernatant was collected and centrifuged at 4 °C and 1000xg for 10 min. A human TGF-β1 enzyme-linked immunosorbent test kit (Cat. No. KGEHC107b-1; KeyGEN Biotech Co., Ltd.) was used to quantify the TGF-β1 levels according to the manufacturer's guidelines.

GEO database analysis

The GSE193258 dataset from the GEO database (https://www.ncbi.nlm.nih.nih.gov/ge/) was selected for this study. The platform used in the GSE193258 dataset was GPL20301, which was analyzed via Illumina's "HiSeq 4000" chip. The original data "GSE193258_RNA-seq_estimated_counts.tsv" were analyzed via R language software, and the "edgeR" package was used to filter low-expression genes on the basis of $|\log \text{fold change}| > 1$ and Benjamini–Hochberg adjusted P value < 0.05. The "Limma" and "Voom" R packages were used to analyze differential expression, and heatmaps and volcano maps were drawn. The "clusterprofiler" R package was used for GO and KEGG enrichment analysis on the basis of the differentially expressed genes.

Quantitative real-time polymerase chain reaction (qRT–PCR)

Total RNA was extracted using the FastPure Cell/Tissue Total RNA Isolation Kit V2 (Cat. No. RC112-01; Vazyme Biotech Co., Ltd.). cDNA synthesis was performed using the HiScript III All-in-One RT SuperMix Perfect for qPCR (Cat. No. R333-01; Vazyme Biotech Co., Ltd.). Quantitative real-time PCR (qRT-PCR) was carried out with the Taq Pro Universal SYBR qPCR Master Mix (Cat. No. Q712-02; Vazyme Biotech Co., Ltd.). All procedures were conducted following the manufacturer's protocols. The primer sequences are shown below.

Primer	Forward	Reverse
YAP	5′-ACAGCAGAACCGTTTCCCAGAC-3′	5′-GACTTGGCATC AGCTCCTCTCC-3′
TAZ	5′-CACGCAGGACCTAGACACAGAC-3′	5′-CAGGATCTTCT TCCGCCACGAG-3′
GAPDH	5′-ACAACTTTGGTATCGTGGAAGG-3′	5′-GCCATCACGCC ACAGTTTC-3′

Knockdown by siRNA

siRNAs for the knockdown of YAP/TAZ were purchased from GeneChem (Shanghai, China). The siRNAs were transfected into H1975 cells for 24 h, and subsequent experiments were performed.

siRNA	Target sequence (5′-3′)	
siYAP-1	5′-CACCGGCACGATCTGATGCCC GGCG-3′	5′-AAACCGCCGGGC ATCAGATCGTGCC-3′
siYAP-2	5′-CACCGGTGCACGATCTGATGC CCGG-3′	5′-AAACCCGGGCAT CAGATCGTGCACC-3′
siTAZ-1	5′-CACCGCGCGAGTGCGAGCCC GAATC-3′	5′-AAACGATTCGGG CTCGCACTCGCGC-3′
siTAZ-2	5′-CACCGGCAAGTGATCCACGTC ACGC-3′	5′-AAACGCGTGACG TGGATCACTTGCC-3′

Survival analysis

The Kaplan–Meier plotter website (https://kmplot.com/analysis/) was used for univariate survival analysis, with an emphasis on overall survival. The median expression level of YAP1 served as the dividing criterion, categorizing lung cancer patients into high and low-expression groups.

Statistical analysis

The data are presented as the means ± SEMs. Each experiment was conducted in triplicate. Group comparisons were performed via Student's t test, and ANOVA of variance was performed via GraphPad software. The standard deviation for statistical significance was set at $P < 0.05$.

Results

Almonertinib significantly inhibited the viability of NSCLC cells

To investigate the sensitivity of different EGFR genotypes to almonertinib, the normal cell line Beas-2B (lung epithelial cells), the lung adenocarcinoma cell line A549 (EGFR wild-type cells), and H1975 (EGFR T790M mutant cells) were treated with 0, 2, 4, 8, 16, or 32 μM almonertinib for 24, 48, or 72 h and subjected to a CCK8 assay. H1975 cells presented the fastest decline in cell viability, followed by A549 cells, whereas Beas-2B cells presented the slowest decline (Fig. 1A). The proliferation, migration, and invasion ability of cells treated with 2.4 μM allorertinib for 24 h were altered in colony formation and transwell invasion assays. When the concentration was increased to 4 μM, 2 μM allorertinib considerably decreased the proliferation, migration, and invasion ability of H1975 cells, and the viability of A549 cells decreased (Fig. 1B-F). Beas-2B cells were largely unaffected by almonertinib treatment. These results showed that almonertinib significantly inhibited the viability of NSCLC cells compared with normal cells, whereas EGFR T790M-mutant cells were more sensitive than were EGFR wild-type cells.

CAFs were successfully induced by TGF-β1

We selected the classical cytokine TGF-β1 (transforming growth factor β1) for the activation of CAFs, which has been confirmed to be associated with the transformation of CAFs in previous studies [15, 16]. Human embryonic HFL1 lung fibroblasts were treated with 10 ng/mL TGF-β1 for 24–48 h for 2–3 passages, and their morphology was observed under a microscope. Normal fibroblasts (NFs) and fibroblasts stimulated with TGF-β1 (CAFs-24 h and CAFs-48 h) for 24 h and 48 h, respectively, did not differ in morphology. Both showed typical fibrocyte-like characteristics, which were flat, spindle shaped, and swirled at dense growth sites (Fig. 2A). α-SMA and FAP expression was evaluated by western blotting. The expression of both markers was greater in the TGF-β1-stimulated fibroblasts than in the NF-stimulated fibroblasts (Fig. 2B). The protein expression levels of α-SMA and FAP in the CAF-48 h group were significantly greater than those in the NF group. However, the differences between the CAF-24 h and NF groups were not statistically significant. The upregulation of CAF markers is an important feature of CAF activation. According to the western blotting results, TGF-β1 successfully induced the conversion of NFs into CAFs. All the CAFs used in the follow-up experiments were obtained from NFs after treatment with TGF-β1 for 48 h.

Almonertinib increased the TGF-β1 secretion of H1975 cells

To detect the secretion of TGF-β1 in EGFR T790M-mutant NSCLC cells before and after almonertinib treatment, the supernatants of H1975 cells treated with 0, 2, or 4 μM almonertinib were collected. The concentration of TGF-β1 in the supernatants of the different groups was determined via an ELISA kit. The amount of TGF-β1 secreted by H1975 cells increased after stimulation with almonertinib (Fig. 2C). Furthermore, the secretion of TGF-β1 in H1975 cells also increased with increasing almonertinib concentration. In addition, H1975 cells themselves do not secrete a small amount of TGF-β1, which supports the use of TGF-β1 as a CAF inducer in this study.

TGF-β1 is a peptide growth factor that has multiple functions. Abnormalities in the signal transduction pathway of TGF-β1 are important factors in cancer development, progression, infiltration, and metastasis. TGF-β1 promotes cell proliferation in progressive tumors, which, in turn, promotes tumor invasion and metastasis. The function of Smad3 is dependent on signal transduction and the regulation of Smad and non-Smad proteins. Notably, Smad3, a major activator of the TGF-β/Smad signaling pathway, regulates gene expression and promotes fibroblast differentiation and proliferation. In addition, TGF-β1, an important member of the TGF-β

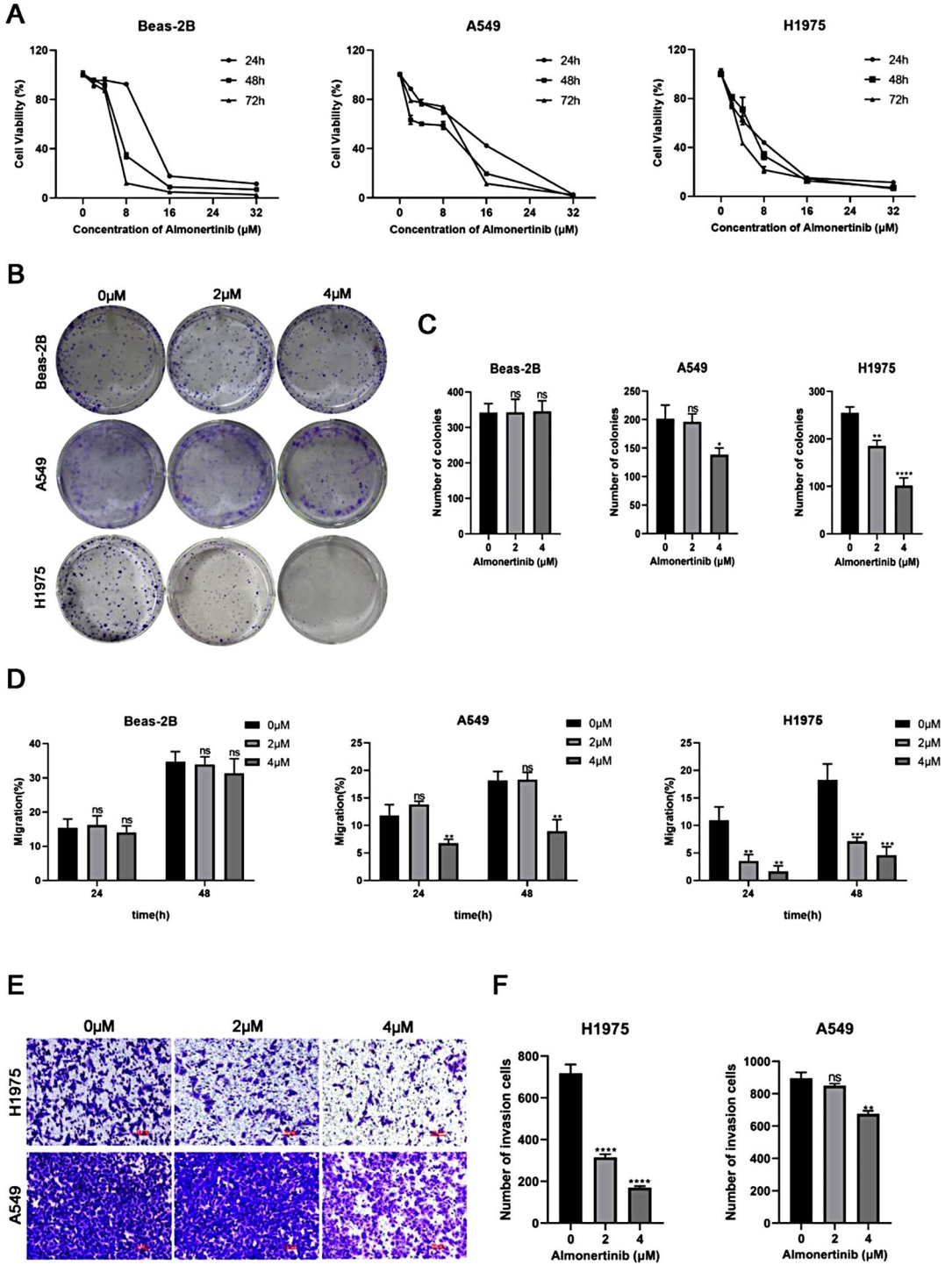

Fig. 1 Almonertinib significantly inhibited the viability of NSCLC cells. (**A**) Beas-2B, A549 and H1975 cells were treated with different concentrations (0, 2, 4, 8, 16, or 32 μM) of almonertinib for 24, 48, or 72 h. Cell viability was measured by a CCK8 assay. Then, Beas-2B, A549 and H1975 cells were treated with 0, 2, or 4 μM almonertinib, respectively. (**B-C**) Colony formation was detected via a colony formation assay. (**D**) Cell migration was evaluated via a wound-healing assay. (**E-F**) Cell invasion was determined by a Transwell invasion assay (magnification, ×100). The values are the means ± SEMs. Significance: ns, not significant; *$p < 0.05$; **$p < 0.01$; ***$p < 0.001$; ****$p < 0.0001$

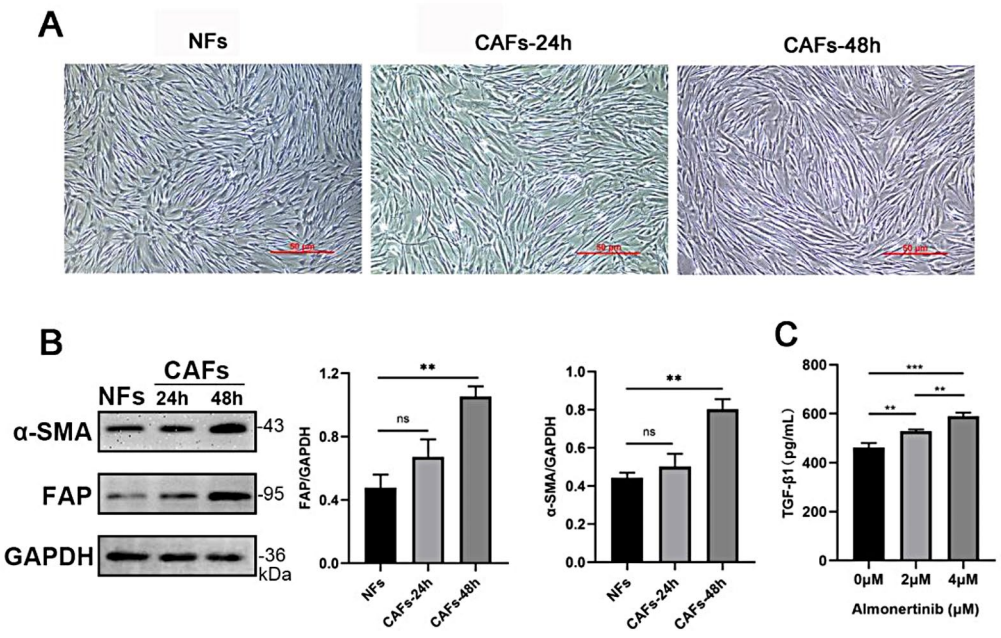

Fig. 2 CAFs were successfully induced by TGF-β1, and almonertinib increased the TGF-β1 secretion of H1975 cells. HFL1 cells were stimulated with 10 ng/mL TGF-β1 for 24–48 h, after which they were passaged 2–3 times. (**A**) Morphology was observed under a microscope (magnification, ×40). (**B**) The expression levels of α-SMA and FAP in the NF, CAF-24 h and CAF-48 h groups were detected by Western blotting. (**C**) The secretion of TGF-β1 in H1975 cells treated with 0, 2, or 4 μM almonertinib was determined by ELISA. The values are the means ± SEMs. Significance: ns, not significant; $^{**}p < 0.01$; $^{***}p < 0.001$

family, has been shown to be a major inducer of EMT and promotes the development of NSCLC. Our experiments revealed that TGF-β1 was induced to convert NFs to CAFs. The secretion of TGF-β1 also increased with increasing almonertinib concentration. Almonertinib may promote the accumulation of CAFs in NSCLC cells by increasing the secretion of TGF-β1. Therefore, we hypothesized that almonertinib may promote tumor development by promoting signaling via the TGF-β1/Smad pathway and inducing the development of epithelial–mesenchymal transition to achieve CAF-induced drug resistance in NSCLC. This hypothesis adds to the possible mechanism underlying the induction of TGF-β1 expression by almonertinib. However, this pathway needs to be further supplemented with relevant experimental validation in subsequently derived subjects to enrich the research.

CAFs alleviated the inhibitory effects of almonertinib on NSCLC cells

CAFs usually promote cancer by secreting various soluble factors and exosomes [17–19]. Therefore, the supernatants of NFs and CAFs collected as conditioned medium (CM) after centrifugation were used to treat H1975 and A549 cells in advance for 48 h. On the basis of previous experimental results, drug concentrations of 2 μM and 4 μM were selected for use in pretreated H1975 and A549 cells, respectively. We used colony formation, Transwell migration, and invasion assays to detect changes in the proliferation, migration, and invasion ability of NSCLC cells treated early with the negative control (NC), NFs, or CAF-CM in the presence of almonertinib. Compared with those of the tumor cells in the NC-CM group, the number of colonies, migration, and invasion of the cells in the CAF-CM group increased at the same drug concentration (Fig. 3). Interestingly, the intervention of NFs with NSCLC cells had a synergistic effect with almonertinib in reducing cell viability. The results showed that after CAF intervention, the survival of NSCLC cells in the presence of almonertinib improved. CAFs alleviated the inhibitory effect of almonertinib on NSCLC cells to a certain extent, whereas NFs had the opposite effect.

The Hippo signaling pathway is correlated with third-generation EGFR-TKI resistance

We selected the GSE193258 dataset from the GEO database, focusing on third-generation EGFR-TKI resistance sequencing, to evaluate the DEGs. The acute group treated with osimertinib for 24 h was considered the osimertinib-sensitive group, and the DTP group treated with osimertinib for 21 days was regarded as the osimertinib-resistant group. The differential expression criteria were determined by $|\log FC| > 1$ and adjusted P value < 0.05 via the Benjamini–Hochberg method.

The data from the acute and DTP groups in the PC9, NCI-H1975, HCC827, and HCC2935 cell lines were analyzed using cell lines as covariates. A total of 393 upregulated and 445 downregulated genes were identified

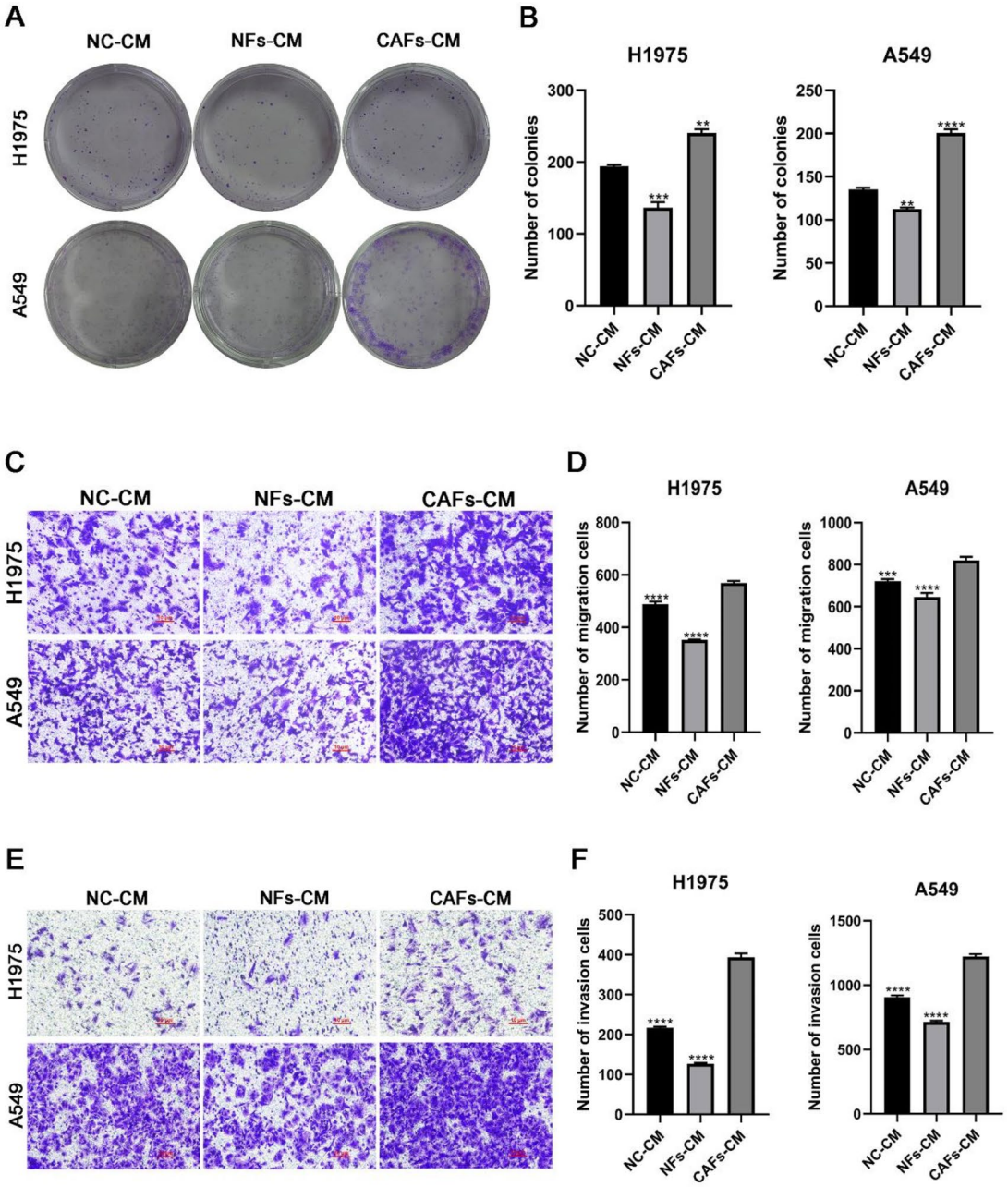

Fig. 3 CAFs alleviated the inhibitory effects of almonertinib on NSCLC cells. The supernatants of NFs and CAFs were centrifuged at 1000xg for 15 min and collected as conditioned medium (CM). H1975 and A549 cells were treated with different CMs for 48 h. Then, they were exposed to 2 or 4 μM almonertinib. (**A-B**) Colony formation was evaluated via a colony formation assay. (**C-D**) Cell migration was determined by a Transwell migration assay (magnification, ×100). (**E-F**) Cell invasion was measured via a Transwell invasion assay (magnification, ×100). The values are the means ± SEMs. Significance: $^{**}p < 0.01$, $^{***}p < 0.001$, $^{****}p < 0.0001$

(Figure S1). Functional enrichment analysis was performed for the downregulated genes; that is, their expression was upregulated in NSCLC cells after the acquisition of osimertinib resistance. GO analysis revealed the top five enrichment pathways of the three functional classifications (BP, CC, and MF), most of which were associated with the extracellular matrix (Figure S2A). KEGG analysis revealed the top 10 enriched pathways, indicating that osimertinib resistance was related to the PI3K/AKT and TGF-β signaling pathways (Figure S2B).

The genes in the acute and DTP groups of H1975 cells were subsequently analyzed for differential expression, and 875 upregulated genes and 538 downregulated genes were screened (Fig. 4A-B). Functional enrichment analysis was subsequently performed for the downregulated genes. GO analysis revealed that the enriched pathways

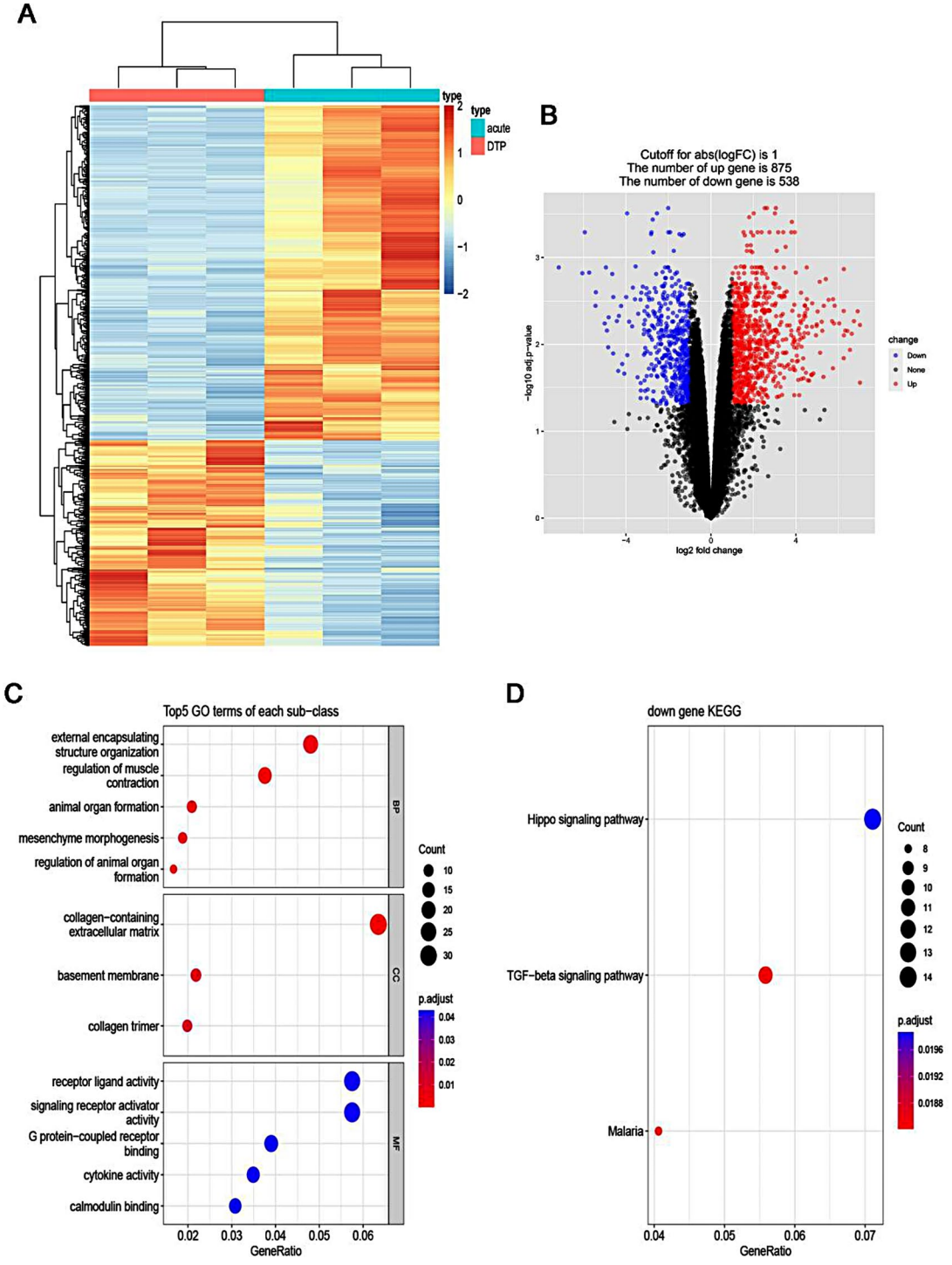

Fig. 4 The Hippo signaling pathway is correlated with third-generation EGFR-TKI resistance. The data from the acute group and DTP group of H1975 cells were analyzed for differential expression. The (**A**) heatmap and (**B**) volcano map are shown. Functional enrichment analysis was subsequently performed for the downregulated genes. The results of (**C**) GO analysis and (**D**) KEGG analysis revealed the top enrichment pathways

were associated with the extracellular matrix and signaling pathway activation, such as external encapsulating structure organization, the collagen-containing extracellular matrix, and receptor ligand activity (Fig. 4C). KEGG analysis identified only three enriched pathways. Among these pathways, the Hippo signaling pathway was the most significant (Fig. 4D). The Hippo signaling pathway is linked to a variety of signaling pathways and has been found to be associated with cell adhesion, tumor growth, and metastasis [20, 21].

These results demonstrate that third-generation EGFR-TKI resistance is correlated with the extracellular matrix and the Hippo signaling pathway.

CAFs downregulated the expression of YAP/TAZ in H1975 cells

YAP/TAZ are the principal molecules of the Hippo pathway and have been demonstrated to be related to CAFs and various physiological functions in tumors [22, 23]. GEPIA2 (http://gepia2.cancer-pku.cn/#index) was used to examine the correlation between YAP1, TAZ, and the CAF marker α-SMA (ACTA2). Both YAP1 and TAZ were weakly and significantly correlated with ACTA2 expression, respectively (Figure S3). YAP/TAZ were further determined to be related to CAFs.

To verify whether the effect of CAFs on NSCLC cells is related to YAP/TAZ, qPCR was used to determine the mRNA expression levels of YAP/TAZ. The YAP/TAZ expression level in EGFR wild-type A549 cells was lower than that in EGFR T790M mutant H1975 cells, which are more sensitive to almonertinib (Fig. 5A). The expression of YAP/TAZ was also downregulated in H1975 cells treated with CAF-CM (Fig. 5B). H1975 cells treated with the negative control or CAF-CM were treated with 2 μM almonertinib for 24 h, and YAP/TAZ expression in the CAF-CM group also decreased (Fig. 5C). Furthermore, we compared the expression of YAP/TAZ in H1975 cells after treatment with CAF-CM untreated with almonertinib and after treatment with 2 μM almonertinib in CAF-CM. Similarly, we discovered that in the presence of almonertinib, CAFs downregulated YAP/TAZ expression levels (Fig. 5D). Combined with the results of previous performance experiments (Figs. 1 and 3), these findings indicate that CAF intervention can downregulate the expression of YAP/TAZ in H1975 cells and that the change in expression may be related to CAF-mediated osimertinib resistance.

YAP1 was associated with poor prognosis in lung cancer patients

Survival analysis of 1,925 lung cancer patients from the TCGA database was performed via the Kaplan–Meier plotter (https://kmplot.com/analysis/) website, with the median YAP1 expression level used as the grouping criterion. The results indicated that the 5-year overall survival rate of patients with low YAP1 expression was lower than that of individuals with high YAP1 expression. Lower YAP1 expression was correlated with unfavorable outcomes in patients with lung cancer (Fig. 5E). This trend was consistent with the results of the functional experiments and qPCR.

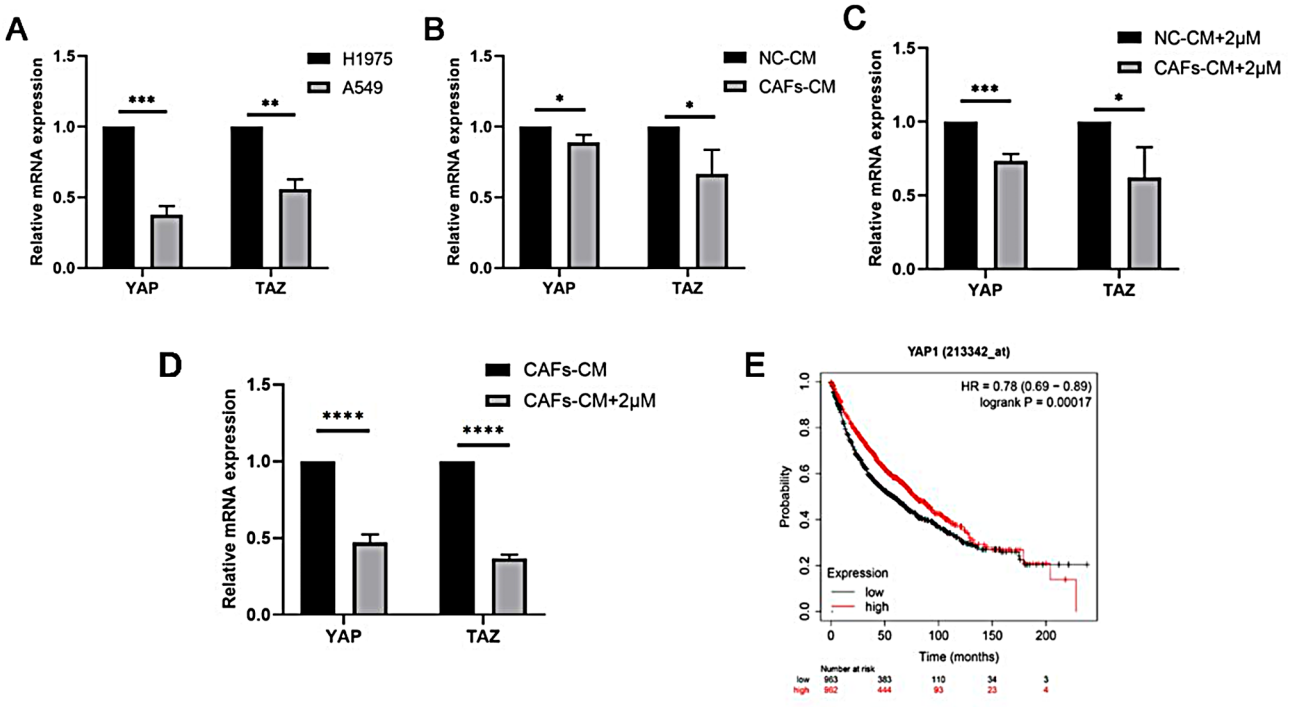

Fig. 5 CAFs downregulated the expression of YAP/TAZ in H1975 cells, and YAP1 was associated with poor prognosis in lung cancer patients. qPCR was used to evaluate the mRNA expression levels of YAP1 and TAZ. Statistical results of YAP/TAZ expression (**A**) in H1975 and A549 cells, (**B**) in H1975 cells treated with NC-CM or CAF-CM and (**C**) then exposed to 2 μM almonertinib for 24 h are represented by bar charts. (**D**) Statistical analysis of YAP/TAZ expression in H1975 cells treated with CAF-CM and H1975 cells exposed to 2 μM almonertinib for 24 h. (**E**) Survival analysis of YAP1 in 1,925 lung cancer patients from the TCGA database was performed. Significance: *$p < 0.05$, **$p < 0.01$, ***$p < 0.001$

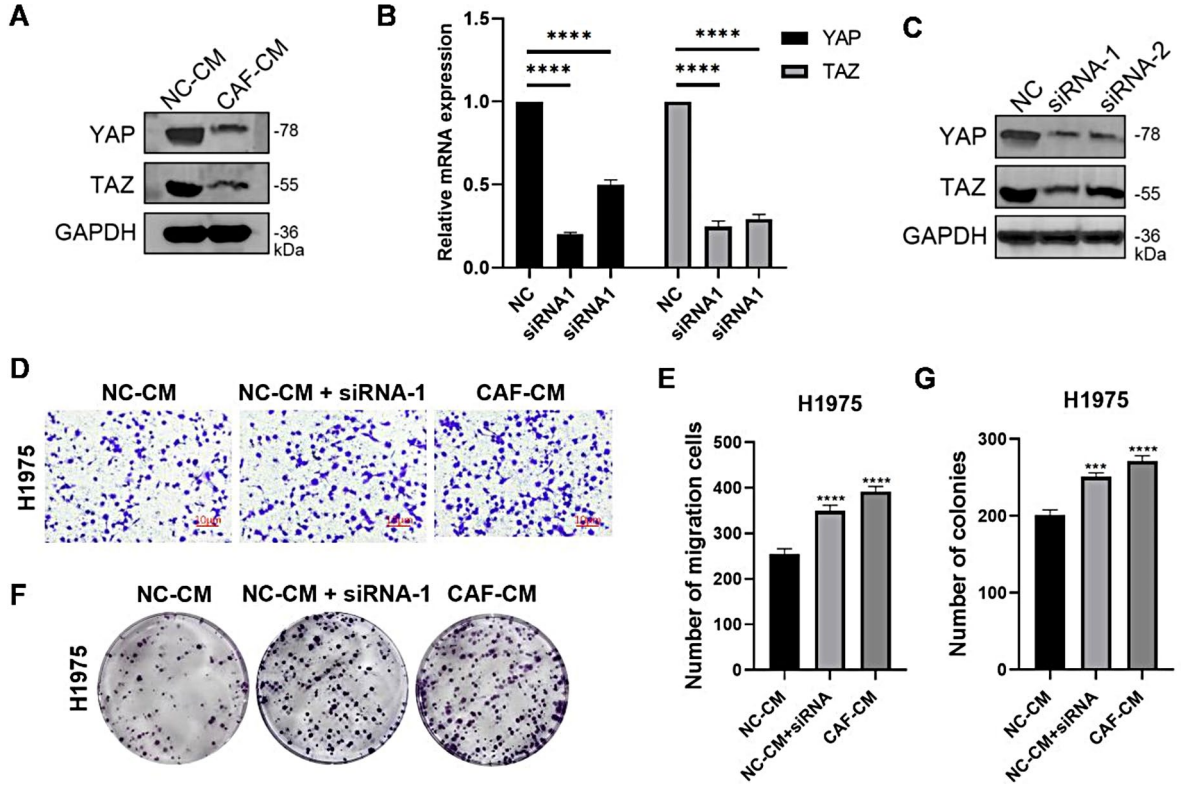

Fig. 6 CAFs influence the YAP/TAZ pathway to facilitate protection of cancer cells from almonertinib drug damage. (**A**) Statistical analysis of YAP/TAZ protein expression in H1975 cells treated with NC-CM or CAF-CM. (**B-C**) Transfection efficiency was verified by qPCR and western blotting after knockdown of YAP/TAZ. (**D-G**) Results of clones and invasion phenotypes of H1975 cells treated with NC-CM, NC-CM + siRNA or CAF-CM. Significance: $^{*}p < 0.05$, $^{**}p < 0.01$, $^{***}p < 0.001$

YAP/TAZ is necessary for the ability of CAFs to protect cancer cells from damage induced by almonertinib

Multiple studies have suggested that the core transduction molecules YAP and TAZ in the Hippo pathway are associated with multiple physiological functions in tumors. On the basis of our previous experimental results, we hypothesized that CAFs promote almonertinib resistance by downregulating YAP/TAZ in lung cancer cells. To validate our hypothesis, we assessed the level of YAP/TAZ expression in cancer cells treated with CAF-CM and observed a significant reduction in YAP/TAZ protein levels compared with those in cells treated with NC-CM (Fig. 6A). This result was consistent with the results of previous qPCR and survival analyses (Fig. 5).

We subsequently knocked down YAP/TAZ expression to investigate whether CAFs contribute to almonertinib resistance in lung cancer. qPCR and western blotting demonstrated that siRNA-1 transfection was more efficient (Fig. 6B-C); therefore, we chose siRNA-1 to confirm that the YAP/TAZ molecular pathway was associated with CAFs to promote NSCLC drug resistance.

Furthermore, we cultured lung cancer cells with CM collected from NC, CAF, or H1975 cells after transfection with siRNA. We found that at the same drug concentration, the number of colonized and invasive cells was greater in both the NC-CM + siRNA group and the CAF-CM group than in the NC-CM-treated group (Fig. 6D-G). The results revealed that the knockdown of YAP/TAZ corresponded to the phenotypic trends observed after intervention with CAFs. These data provide evidence that CAFs protect cancer cells from almonertinib drug damage by downregulating YAP/TAZ in lung cancer cells.

Discussion

Although it was approved in China after osimertinib, almonertinib is the second third-generation EGFR-TKI and the first to be manufactured domestically. It was first sanctioned as second-line therapy for patients with NSCLC who had received prior treatment with EGFR-TKIs and whose condition worsened during or after treatment for EGFR T790M-positive mutations [24]. In December 2021, almonertinib received official approval for adult patients with advanced or metastatic NSCLC exhibiting EGFR exon 19 deletions or exon 21 L858R point mutations [25]. Thus, almonertinib is suitable for the treatment of patients with EGFR-activating mutations or T790M-resistant mutations, which is consistent with the findings of this study.

In this study, the normal lung epithelial cell line Beas-2B, the lung adenocarcinoma cell line EGFR wild-type

A549, and the EGFR T790M mutant H1975 cell line were selected as study subjects, and the cytotoxicity of almonertinib was detected via the CCK8 assay. The three cell lines presented different sensitivities to almonertinib, but cell viability varied in a time- and concentration-dependent manner. Next, 2 μM and 4 μM almonertinib were selected to treat the cells in the low- and high-concentration almonertinib stimulation groups, respectively. Almonertinib dramatically reduced the proliferation, migration, and invasion of EGFR T790M-mutant H1975 cells. High concentrations of almonertinib inhibited EGFR wild-type A549 cells to a certain extent, whereas normal EGFR wild-type Beas-2B cells were mostly unaffected by almonertinib. This may be because although the inactive conformation of wild-type EGFR is poorly bound to almonertinib, the two still bind when the concentration of almonertinib increases, and the EGFR expression level in normal cells is lower than that in tumor cells.

Because of the difficulty in collecting EGFR T790M-mutant NSCLC tissue samples, we selected TGF-β1 as the CAF activator. Transforming growth factor beta 1 (TGF-β1) is a classic cytokine that is a member of the TGF-β family and is involved in multiple biological functions, such as cell proliferation, organization development, and embryo differentiation [26–28]. It was originally isolated from serum to induce fibroblast transformation and adherent-independent growth, together with epidermal growth factor. It was later reported that TGF-β1 is a bifocal regulator that can promote or inhibit cell proliferation depending on environmental conditions [29, 30]. TGF-β1 is expressed in almost all cells, including tumor cells and cancer-associated fibroblasts, and promotes fibrosis in a variety of tissues, such as the lungs, liver, and heart [31–33]. The characterization of fibroblasts stimulated with TGF-β1 revealed that the cell morphology did not change after TGF-β1 stimulation, while the expression of the CAF markers α-SMA and FAP was upregulated, confirming that TGF-β1 successfully induced CAF transformation.

To further support the use of TGF-β1 as a CAF inducer, the TGF-β1 content in H1975 cells before and after almonertinib treatment was detected via ELISA. The results showed that the secretion of TGF-β1 by H1975 cells increased with increasing concentrations of almonertinib. These findings suggest that while inhibiting the viability of NSCLC cells, almonertinib may promote the accumulation of CAFs due to increased secretion of TGF-β1, resulting in extracellular matrix deposition.

Studies to date have shown that CAFs are not only involved in promoting the occurrence and development of tumors but also induce tumor drug resistance through various mechanisms. CAFs can secrete exosomes and soluble factors to activate signaling pathways in tumor cells, reshape the extracellular matrix, and generate an immunosuppressive microenvironment, thereby affecting the sensitivity of tumor cells to antitumor drugs. CAFs secrete exosomes containing miRNA-130a and deliver them to NSCLC cells to promote cisplatin resistance [17]. In lung squamous cell carcinoma, CAFs recruit CCR2 + monocytes via CCL2 and induce their differentiation into the myeloid-derived suppressor cell (MDSC) phenotype, where MDSCs generate reactive oxygen species and create an immunosuppressive microenvironment [34]. CAFs secrete HGF and IGF-1, which bind to their corresponding receptors on NSCLC cells, upregulate the expression of intracellular ANXA2, and induce insensitivity to gefitinib [13]. However, the relationship between CAFs and the third-generation EGFR-TKI almonertinib is unclear.

After successful induction and verification, the CM of NFs and CAFs was collected, and H1975 and A549 cells were pretreated and then treated with 2 μM and 4 μM almonertinib, respectively, to detect changes in viability. The inhibition of the proliferation, migration, and invasion of NSCLC cells treated with CAF-CM was alleviated in the presence of almonertinib. These findings suggest that CAFs increase the tolerance of NSCLC cells to almonertinib and induce almonertinib resistance. This may be related to soluble cytokines secreted by CAFs through the activation of relevant signaling pathways in NSCLC cells. The common signaling pathways associated with CAFs and tumor resistance include the MAPK, JAK/STAT, and PI3K/AKT/mTOR pathways [35–37]. For example, in a neuroblastoma mouse model, inhibition of the JAK2/STAT3 and MEK/ERK/1/2 pathways increased tumor sensitivity to etoposide, limited the carcinogenic activity of mesenchymal stromal cells, and inhibited tumor progression [38]. However, CAFs are involved in many signaling pathways, and the mechanism by which CAFs induce almonertinib resistance remains to be explored. In addition, compared with those in the CAF-CM group, the viability of NSCLC cells treated with NF-CM was weakened in combination with NFs and almonertinib, which may be related to phenotypic changes in NFs and CAFs.

Owing to the lack of sequencing data on almonertinib resistance, we selected the GSE193258 dataset as the analysis object, screened the genes differentially expressed between the osimertinib-sensitive (acute group) and osimertinib-resistant (DTP group) groups, and then performed GO and KEGG enrichment analyses. GEO data analysis revealed that third-generation EGFR-TKI resistance is associated with the extracellular matrix and the Hippo signaling pathway. CAFs regulate extracellular matrix components to a large extent, and the Hippo signaling pathway is known to be related to CAFs.

The Hippo signaling pathway consists of a cascade of signals involved in various biological functions [39]. The

main components of the Hippo pathway are the kinase cascade MST1/2, LATS1/2, the transcriptional activator YAP/TAZ, and downstream effector molecules. The transcriptional activator YAP/TAZ is phosphorylated by the LATS1/2 kinase, which is activated by the MST1/2 kinase when it phosphorylates the LATS1/2 kinase [40]. YAP/TAZ are two highly related transcriptional activators that are expressed in a variety of solid tumors; these activators do not contain DNA-binding domains and cannot bind to DNA; therefore, they regulate cell physiological functions by translocating from the cytoplasm to the nucleus and binding to DNA-binding transcription factors [41–43]. Because activated YAP/TAZ molecules are unable to undergo nuclear translocation, they remain in the cytoplasm, bind to 14-3-3 or ubiquitinate, and are degraded by proteasomes. More importantly, in addition to its effect on the viability of tumor cells, YAP affects the function of CAFs. In breast cancer, CAFs require YAP to promote increased matrix rigidity, cancer cell invasion, and angiogenesis, which are related to the regulation of the expression of multiple cytoskeletal regulatory factors by YAP [44]. The activation of YAP transcription factors is considered a signature feature of CAFs [45].

We used the GEPIA2 website to determine a weakly significant association between YAP1, TAZ, and the CAF marker α-SMA (ACTA2), which was subsequently verified by qPCR. The results revealed that the expression level of YAP/TAZ in EGFR wild-type A549 cells was lower than that in EGFR T790M mutant H1975 cells and that CAF intervention reduced the expression of YAP/TAZ in H1975 cells in the presence or absence of almonertinib. These findings suggest that the mechanism by which CAFs induce almonertinib resistance may be related to YAP/TAZ. Moreover, survival analysis revealed that low YAP1 expression is associated with poor prognosis in patients with lung cancer. Next, we verified the above qPCR and bioinformatics analysis results via western blotting. We hypothesized that the YAP/TAZ molecular pathway is associated with CAFs to promote drug resistance in NSCLC. To verify our hypothesis, we evaluated the phenotypic effects of YAP/TAZ knockdown in NC-CM-, NC-CM-siRNA-, and CAF-CM-treated cancer cells. These results confirmed that CAFs protect cancer cells from almonertinib drug damage through the downregulation of YAP/TAZ in lung cancer cells. Since YAP/TAZ functions mainly through nuclear translocation, exploring its function in signal transduction requires assessing its phosphorylation gravity or intracellular localization. Therefore, subsequent experiments can detect phosphorylated YAP/TAZ by western blotting or locate YAP/TAZ by immunohistochemistry or immunofluorescence and detect the expression of related downstream genes to further explore the specific mechanism involved.

Notably, our research has several limitations. Importantly, the public dataset contained a limited amount of data. Therefore, the survival-related clinical data obtained from the database in this study are not exhaustive and may lead to errors or biases. In addition, we are actively validating clinical patient-related experiments, but the sample size is insufficient because of the low number of patients who currently satisfy the inclusion criteria in the hospital. In future research, we will expand the sample size to reduce bias and confirm the results. Therefore, the clinical aspects of the validation results can be completed and added to subsequent extension work. In addition, further validation of the relationship between CAFs and osimertinib resistance in vivo is needed to confirm our findings. Finally, the results of this research may not be applicable to patients in Asian countries, as all downloaded datasets used for survival analyses were from Western countries. Additional investigations are needed to validate these findings.

Conclusion

In conclusion, almonertinib significantly inhibited the proliferation, migration, and invasion of EGFR T790M-mutant NSCLC cells. H1975 cells stimulated with almonertinib may promote the accumulation of CAFs in NSCLC cells by increasing the secretion of TGF-β1. CAFs can improve the survival of NSCLC cells treated with almonertinib and induce almonertinib resistance. The Hippo signaling pathway has been confirmed to be associated with third-generation EGFR-TKI resistance, and the induction of osimertinib resistance in NSCLC cells by CAFs may be related to YAP/TAZ.

Supplementary Information

The online version contains supplementary material available at https://doi.org/10.1186/s12967-024-06064-z.

Supplementary Material 1: Figure S1. There were 393 upregulated genes and 445 downregulated genes in the acute group and DTP group in the PC9, NCI-H1975, HCC827, and HCC2935 cell lines when the cell lines were used as covariates. The (A) heatmap and (B) volcano map are shown. Figure S2. Functional enrichment analysis was subsequently performed for the downregulated genes. The results of (A) GO analysis and (B) KEGG analysis revealed the top enrichment pathways. Figure S3. YAP1 and TAZ were weakly and significantly correlated with ACTA2. The GEPIA2 website was used to analyze the correlations between (A) YAP1 or (B) TAZ and the CAF marker α-SMA (ACTA2).

Acknowledgements

We acknowledge the TCGA and GEO databases for providing their platforms and contributors for uploading meaningful datasets.

Author contributions

Guohao Wei, Yu Nie, wrote the article; Guohao Wei and Yu Nie completed the relevant experiments together; Guohao Wei, Yu Nie, Ming Sun and Wenzheng Zhou both designed the experiment and contributed to the resources; Huihui Zhao, Fangfang Chen and Chuandong Zhu analyzed data; Chuandong Zhu administrated the whole study.

Funding
This study was funded by the Nanjing Medical Science and Technology Development Project (ZKX23037), Nanjing Second Hospital Talent Support Project (RCZD202302), Natural Science Foundation of Nanjing University of Chinese Medicine (XRZ2021078), National Health and Wellness Commission's Special Project for Post-marketing Clinical Research of Innovative Drugs (WKZX2024CX101211), Special Grant for Clinical Research of Wu Jieping Medical Foundation (320.6750.2023-17-2), and Postgraduate Research & Practice Innovation Program of Jiangsu Province (KYCX23_2105).

Data availability
The datasets generated and/or analyzed during the current study are available from the corresponding author upon reasonable request.

Declarations

Ethics approval and consent to participate
Not applicable.

Consent for publication
The authors have consent for publication.

Competing interests
The authors have no competing interests.

Author details
[1]Department of Oncology, The Second Hospital of Nanjing, Affiliated to Nanjing University of Chinese Medicine, Nanjing 210003, China
[2]Department of Clinical Laboratory, Jinling Hospital, Affiliated Hospital of Medical School, Nanjing University, Nanjing 210002, China
[3]Department of Oncology, The Second Hospital of Nanjing, Nanjing University of Chinese Medicine, Nanjing 210003, China

Received: 14 August 2024 / Accepted: 28 December 2024
Published online: 10 January 2025

References

1. Siegel RL, Miller K D Waglens, et al. Cancer statistics, 2023 [J]. Cancer J Clin. 2023;73(1):17–48.
2. RECK M, CARBONE D P, GARASSINO M, et al. Targeting KRAS in non-small-cell lung cancer: recent progress and new approaches [J]. Annals Oncology: Official J Eur Soc Med Oncol. 2021;32(9):1101–10.
3. POPAT S, HSIA T C, HUNG J Y, et al. Tyrosine kinase inhibitor activity in patients with NSCLC harboring uncommon EGFR mutations: a Retrospective International Cohort Study (UpSwinG) [J]. Oncologist. 2022;27(4):255–65.
4. DONG R F, ZHU M L, LIU M M, et al. EGFR mutation mediates resistance to EGFR tyrosine kinase inhibitors in NSCLC: from molecular mechanisms to clinical research [J]. Pharmacol Res. 2021;167:105583.
5. FU K, XIE F, WANG F, et al. Therapeutic strategies for EGFR-mutated non-small cell lung cancer patients with osimertinib resistance [J]. J Hematol Oncol. 2022;15(1):173.
6. BENJAMIN D J NAGASAKAM. Freeing the competition: will Aumolertinib (AENEAS) have a fighting chance against Osimertinib (FLAURA)? [J]. J Clin Oncol. 2023;41(4):742–4.
7. YOSAATMADJA Y, SILVA S, DICKSON JM, et al. Binding mode of the breakthrough inhibitor AZD9291 to epidermal growth factor receptor revealed [J]. J Struct Biol. 2015;192(3):539–44.
8. CHEN Y, ZHU S, LIU T et al. Epithelial cells activate fibroblasts to promote esophageal cancer development [J]. Cancer Cell, 2023, 41(5): 903 – 18.e8.
9. MAK TK, LI X, HUANG H, et al. The cancer-associated fibroblast-related signature predicts prognosis and indicates immune microenvironment infiltration in gastric cancer [J]. Front Immunol. 2022;13:951214.
10. HERRERA M, BERRAL-GONZ LEZ A, L PEZ-CADE I, et al. Cancer-associated fibroblast-derived gene signatures determine prognosis in colon cancer patients [J]. Mol Cancer. 2021;20(1):73.
11. KILVAER T K, KHANEHKENARI M R, HELLEVIK T, et al. Cancer Associated fibroblasts in stage I-IIIA NSCLC: prognostic impact and their correlations with Tumor Molecular markers [J]. PLoS ONE. 2015;10(8):e0134965.
12. WANG B, LIU W, LIU C, et al. Cancer-Associated fibroblasts promote Radioresistance of breast Cancer cells via the HGF/c-Met Signaling pathway [J]. Int J Radiat Oncol Biol Phys. 2023;116(3):640–54.
13. WANANDI S I, HILBERTINA N, SIREGAR NC, et al. Cancer-associated fibroblast (CAF) secretomes-induced epithelial-mesenchymal transition on HT-29 colorectal carcinoma cells associated with hepatocyte growth factor (HGF) signalling [J]. JPMA J Pakistan Med Association. 2021;71(Suppl 2):S18–24.
14. QIN H, YANG Y, JIANG B, et al. SOX9 in prostate cancer is upregulated by cancer-associated fibroblasts to promote tumor progression through HGF/c-Met-FRA1 signaling [J]. FEBS J. 2021;288(18):5406–29.
15. TAN H X, XIAO Z G, HUANG T, et al. CXCR4/TGF-β1 mediated self-differentiation of human mesenchymal stem cells to carcinoma-associated fibroblasts and promoted colorectal carcinoma development [J]. Cancer Biol Ther. 2020;21(3):248–57.
16. WANG B, ZHANG S, TONG F, et al. HPV(+) HNSCC-derived exosomal mir-9-5p inhibits TGF-β signaling-mediated fibroblast phenotypic transformation through NOX4 [J]. Cancer Sci. 2022;113(4):1475–87.
17. ZHANG T, ZHANG P, LI HX. CAFs-Derived exosomal miRNA-130a confers Cisplatin Resistance of NSCLC cells through PUM2-Dependent packaging [J]. Int J Nanomed. 2021;16:561–77.
18. MA Z, LI X, MAO Y, et al. Interferon-dependent SLC14A1(+) cancer-associated fibroblasts promote cancer stemness via WNT5A in bladder cancer [J]. Cancer Cell. 2022;40(12):1550–e657.
19. ZHANG C, WANG X Y, ZHANG P, et al. Cancer-derived exosomal HSPC111 promotes colorectal cancer liver metastasis by reprogramming lipid metabolism in cancer-associated fibroblasts [J]. Volume 13. Cell death & disease; 2022. p. 57. 1.
20. XIONG Y, DONG L, BAI Y, et al. Piezo1 activation facilitates ovarian cancer metastasis via Hippo/YAP signaling axis [J]. Channels (Austin Tex). 2022;16(1):159–66.
21. YU B, SU J, SHI Q, et al. KMT5A-methylated SNIP1 promotes triple-negative breast cancer metastasis by activating YAP signaling [J]. Nat Commun. 2022;13(1):2192.
22. XU C, JIN G, WU H, et al. SIRPγ-expressing cancer stem-like cells promote immune escape of lung cancer via Hippo signaling [J]. J Clin Investig. 2022;132(5):e141797.
23. YOU W, DI A, ZHANG L, et al. Effects of wogonin on the growth and metastasis of colon cancer through the Hippo signaling pathway [J]. Bioengineered. 2022;13(2):2586–97.
24. LU S, WANG Q, ZHANG G, et al. Efficacy of Aumolertinib (HS-10296) in patients with Advanced EGFR T790M + NSCLC: updated Post-national Medical products Administration approval results from the APOLLO Registrational trial [J]. J Thorac Oncology: Official Publication Int Association Study Lung Cancer. 2022;17(3):411–22.
25. LU S, DONG X. AENEAS: a Randomized Phase III Trial of Aumolertinib Versus Gefitinib as First-Line therapy for locally Advanced or MetastaticNon-Small-Cell Lung Cancer with EGFR exon 19 deletion or L858R mutations [J]. J Clin Oncol. 2022;40(27):3162–71.
26. YING H, FANG M, HANG Q Q, et al. Pirfenidone modulates macrophage polarization and ameliorates radiation-induced lung fibrosis by inhibiting the TGF-β1/Smad3 pathway [J]. J Cell Mol Med. 2021;25(18):8662–75.
27. ZHANG J, JIANG N, PING J, et al. TGF–β1–induced autophagy activates hepatic stellate cells via the ERK and JNK signaling pathways [J]. Int J Mol Med. 2021;47(1):256–66.
28. XIAO H, ZHANG T, LI C, et al. Mechanical stimulation promotes enthesis injury repair by mobilizing Prrx1(+) cells via ciliary TGF-β signaling [J]. eLife. 2022;11:e73614.
29. LI J, GE L, ZHAO Y, et al. TGF-β2 and TGF-β1 differentially regulate the odontogenic and osteogenic differentiation of mesenchymal stem cells [J]. Arch Oral Biol. 2022;135:105357.
30. PINKAEW D, MARTINEZ-HACKERT E, JIA W, et al. Fortilin interacts with TGF-β1 and prevents TGF-β receptor activation [J]. Commun Biology. 2022;5(1):157.
31. WANG J, LAI X. Nestin promotes pulmonary fibrosis via facilitating recycling of TGF-β receptor I [J]. Eur Respir J. 2022;59(5):2003721.
32. HU YANJ, SHI B. Gli2-regulated activation of hepatic stellate cells and liver fibrosis by TGF-β signaling [J]. Am J Physiol Gastrointest Liver Physiol. 2021;320(5):G720–8.
33. DZIAŁO E, CZEPIEL M, TKACZ K, et al. WNT/β-Catenin signaling promotes TGF-β-Mediated activation of human cardiac fibroblasts by enhancing IL-11 production [J]. Int J Mol Sci. 2021;22(18):10072.

34. XIANG H, RAMIL C P, HAI J, et al. Cancer-Associated fibroblasts promote immunosuppression by inducing ROS-Generating Monocytic MDSCs in Lung squamous cell carcinoma [J]. Cancer Immunol Res. 2020;8(4):436–50.
35. WU F, YANG J, LIU J, et al. Signaling pathways in cancer-associated fibroblasts and targeted therapy for cancer [J]. Volume 6. Signal transduction and targeted therapy; 2021. p. 218. 1.
36. JIA C, WANG G, WANG T, et al. Cancer-associated fibroblasts induce epithelial-mesenchymal transition via the transglutaminase 2-dependent IL-6/IL6R/STAT3 axis in Hepatocellular Carcinoma [J]. Int J Biol Sci. 2020;16(14):2542–58.
37. MA Y, ZHU J, CHEN S, et al. Low expression of SPARC in gastric cancer-associated fibroblasts leads to stemness transformation and 5-fluorouracil resistance in gastric cancer [J]. Cancer Cell Int. 2019;19:137.
38. BORRIELLO L, NAKATA R, SHEARD MA, et al. Cancer-Associated fibroblasts share characteristics and protumorigenic activity with mesenchymal stromal cells [J]. Cancer Res. 2017;77(18):5142–57.
39. LI FL, FU V, LIU G, et al. Hippo pathway regulation by phosphatidylinositol transfer protein and phosphoinositides [J]. Nat Chem Biol. 2022;18(10):1076–86.
40. HAN H, NAKAOKA H J HOFMANNL, et al. The Hippo pathway kinases LATS1 and LATS2 attenuate cellular responses to heavy metals through phosphorylating MTF1 [J]. Nat Cell Biol. 2022;24(1):74–87.
41. ONG Y T, ANDRADE J, ARMBRUSTER M, et al. A YAP/TAZ-TEAD signalling module links endothelial nutrient acquisition to angiogenic growth [J]. Nat Metabolism. 2022;4(6):672–82.
42. LI H, WU B K, KANCHWALA M, et al. YAP/TAZ drives cell proliferation and tumour growth via a polyamine-eIF5A hypusination-LSD1 axis [J]. Nat Cell Biol. 2022;24(3):373–83.
43. SHEN Y, WANG X, LIU Y, et al. STAT3-YAP/TAZ signaling in endothelial cells promotes tumor angiogenesis [J]. Sci Signal. 2021;14(712):eabj8393.
44. CALVO F, EGE N, GRANDE-GARCIA A, et al. Mechanotransduction and YAP-dependent matrix remodelling is required for the generation and maintenance of cancer-associated fibroblasts [J]. Nat Cell Biol. 2013;15(6):637–46.
45. LEE PJ, SUI Y H, LIU T T, et al. Epstein-Barr viral product-containing exosomes promote fibrosis and nasopharyngeal carcinoma progression through activation of YAP1/FAPα signaling in fibroblasts [J]. J Experimental Clin cancer Research: CR. 2022;41(1):254.

Publisher's note